

Cooperative epidemics on multiplex networks

N. Azimi-Tafreshi

Physics Department, Institute for Advanced Studies in Basic Sciences, 45195-1159 Zanzan, Iran

The spread of one disease, in some cases, can stimulate the spreading of another infectious disease. Here, we treat analytically a symmetric co-infection model for spreading of two diseases on a 2-layer multiplex network. We allow layer overlapping, but we assume that each layer is random and locally loop-less. Infection with one of the diseases increases the probability to get infected by the other. Using generating function method, we calculate exactly the fraction of individuals infected with both diseases (so-called co-infected clusters) in the stationary state, as well as the epidemic spreading thresholds and the phase diagram of the model. With increasing cooperation, we observe a tricritical point and the type of transition changes from continuous to hybrid. Finally we compare the co-infected clusters in the case of co-operating diseases with the so-called “viable” clusters in networks with dependencies.

PACS numbers: 89.75.Hc, 87.19.Xx, 05.70.Fh, 64.60.ah

I. INTRODUCTION

Cooperation between two epidemics occurs when the spread of one disease increases the spreading of the other. It was estimated in 2011 [1] that out of a total world population of 7 billion people, less than 2 per mile had active tuberculosis (TB). But if one restricted oneself to the ~ 33 million people with human immunodeficiency virus (HIV), about 30% had also active or latent TB. Inversely, out of the active TB cases, about 15 % had also HIV, which is nearly a factor 100 higher than the incidence rate in the total population. People with HIV and TB co-infection typically also experience faster disease progression than those with TB or HIV alone. Another dramatic example where two diseases mutually enhance their spreading is HIV and the hepatitis C virus (HCV)[2]. Also there, it is estimated that about one third of all people with HIV are also co-infected with HCV.

These numbers show already that mutual co-infection is a huge problem. But there are also other recent examples like HIV and hepatitis B [3], while historically the case of Spanish flu and TB was one of the most devastating [4].

Therefore, much effort recently has been devoted to studying the dynamics of spreading of two or more co-operating pathogens [5–11]. Let us just discuss a few of these papers. Newman *et al.* [6] assumed an asymmetric rule for cooperation, such that the first disease spreads independently of the second one, but the second can propagate only among those that had already been infected with the first disease. This simplifies of course the analysis, but prevents the most dramatic scenarios that may occur if the cooperation is mutual and symmetric, as assumed in [7, 8]. There, each disease can spread independently of the other, but the secondary infection rates are enhanced as compared to the rates for infection by the first diseases. Such a model was treated in mean field theory in [7], while detailed simulations on various types of networks are reported in [8].

The main result of [8] was that the typical “continuous” phase transition observed in simple epidemic models

can be replaced – depending on details of the networks and of the infection processes – by “discontinuous” ones, where the incidence rate at threshold does not increase continuously but jumps immediately to a finite value. In typical discontinuous (or “first order”) phase transitions, there is no sign of warning – like enhanced fluctuations, an increasing correlation length or a slowing down of the dynamics, that occur in single epidemics [12] – as the threshold for large-scale spreading is approached. This is of course the most worrying aspect for health policies, but fortunately most of the discontinuous transitions found in [8] were “hybrid”, i.e. they combined the jumps of first order transitions with the anomalies in the approach to the threshold seen in continuous (or “second order”) transitions.

The results of [5–11] are extremely interesting, but most were obtained either by some sort of mean field theory (i.e., all network properties were neglected and/or stochastic fluctuations are assumed to be absent) or by simulating very specific cases. The range of phenomena found in [8] strongly suggests that one should look for analytic results that do take into account fluctuations and at least some simple network structure.

This is the main aim of the present paper. Another aim is to understand the links between co-infections and catastrophic cascades on networks with interdependencies [13]. The latter can be understood most easily [14–18] as “viable” clusters on multiplex networks. Multiplex networks [19, 20] are a set of nodes interlinked by several (two in the cases discussed here) sets of links, where each type of link allows for the spreading of one of two types of agents. A cluster on such a network is called viable [15], if each of its nodes can be reached from any other node by both types of agents. Obviously there is an analogy with cooperating coinfections, if we identify the two agents with the two pathogens: In the limit of strong cooperativity, large infected clusters will always be coinfecting, i.e. each node on such a cluster will be reachable by both pathogens propagating only on the cluster. But the detailed nature of this connection has remained elusive up to now. It will be clarified in the present paper.

Finally, we should also point out that the case of co-operating epidemics is very much different from the case of competing or antagonistic epidemics [21–30]. Although the latter are also of huge practical interest, their dynamics is very different and leads in general to less dramatic effects.

The paper is organized as follows. In the next section, we introduce a co-infection model on a multiplex network with two types of edges and present an analytical framework enabling us to describe the nature of the transitions corresponding to the emergence of co-infected clusters. We apply our general results to the Erdős–Rényi multiplex networks. The paper concluded in Sec. III.

II. COOPERATIVE EPIDEMICS

A. Analytical framework

Let us consider an uncorrelated multiplex network having two types of edges $i = a, b$. The network can be treated as a superposition of two network layers with edges of type a and b , such that overlapping of two types of edges can exist for some pairs of nodes. The multiplex network is completely described by the joint degree distribution $P(k_a, k_b, k_{ab})$, in which k_i and k_{ab} denote the degree for edges of type i and overlapped edges, respectively.

A co-infection model is defined for two diseases a and b , spreading on the multiplex network. Each of i diseases spreads with transmission probability T_i through only edges of type i , while the overlapped edges can transmit both diseases with probability T_{ab} . We assume that both diseases follow the susceptible–infective–recovered (SIR) dynamics [31]. A given random node can be infected with disease i , if it has at least one edge of type i , connecting it to its infected neighbors. We assume that during the spreading process, if a node can receive both diseases, each one through at least one edge of each type i , it receives the diseases with more probability, such that the transmissibilities T_a and T_b are increased by factor $\alpha > 1$. Also, through the overlapped edges both diseases can be transmitted with the enhanced transmissibility $T_{ab} > T_a T_b$.

It was shown that there is a mapping between the SIR epidemic model and bond percolation theory, such that the set of individuals infected by a disease outbreak with transmissibility T , has the same size as the giant connected cluster of occupied edges with the occupation probability T [12, 32]. Hence, using percolation theory and the generation function method, we can solve exactly for the fraction of individuals, infected by both diseases on configuration model networks with arbitrary degree distributions.

Those nodes connected with the occupied overlapped edges can behave as a whole, since if one of them is infected by both diseases, all others will also be infected. Hence we can merge these nodes into a single node, so-

called a supernode [33, 34]. On the other word, the network is renormalized to a network with supernodes connected with only the non-overlapped edges. One can find the probability that a random node belongs to a supernode with size m , denoted by $R(m, T_{ab})$ [35]. Assuming, there is no correlation between the overlapped and non-overlapped edges in the original network, namely $P(k_a, k_b, k_{ab}) = P(k_a, k_b)P(k_{ab})$, the size distribution of the supernodes is obtained for every arbitrary overlapping degree distribution $P(k_{ab})$,

$$R(m, T_{ab}) = \frac{T_{ab}^{m-1} \langle k_{ab} \rangle}{(m-1)!} \left[\frac{d^{m-2}}{dx^{m-2}} [G_1(x)]^m \right]_{x=1-T_{ab}} \quad (1)$$

In which $G_1(x)$ is the generation function for the distribution of the overlapped degrees of nodes, reached by following a randomly chosen overlapped edge and is given by [36],

$$G_1(x) = \sum_{k_{ab}} \frac{k_{ab} P(k_{ab})}{\langle k_{ab} \rangle} x^{k_{ab}-1}. \quad (2)$$

We define $\mathbf{q} \equiv (q_a, q_b)$ as degree of supernodes which denotes the number of non-overlapped edges of each supernode. From renormalization theory, degree distribution of supernodes with size m , $P_m(\mathbf{q})$ is determined as the distribution of sum of m random variables chosen from the marginal (non-overlapped) degree distribution $P(k_a, k_b)$, which is m -th order convolution of $P(k_a, k_b)$ [37].

To find the size of the giant co-infected cluster, for each type $i = a, b$ of edge we define x_i to be the probability that the end node (supernode) of a randomly chosen edge of type i is the root of an infinite sub-tree infected with disease i . The subtree infected with disease i , by definition means that the subtree's nodes have disease i , but they can have the other disease or not. The probabilities x_a and x_b , are schematically showed in Fig. 1. These probabilities play the role of the order parameters of the phase transition associated with the emergence of the giant co-infected cluster. We can write the self-consistency equations for probabilities x_i using the locally treelike structure of the renormalized networks,

$$x_i = R_\infty + \sum_{m=1}^{\infty} R(m, T_{ab}) \sum_{\mathbf{q}} \frac{q_i P_m(\mathbf{q})}{\langle q_i \rangle} \times \left(\left[1 - (1 - \alpha T_i x_i)^{q_i-1} \right] \left[1 - (1 - \alpha T_j x_j)^{q_j} \right] + p \left[1 - (1 - T_i x_i)^{q_i-1} \right] (1 - T_j x_j)^{q_j} \right). \quad (3)$$

Where R_∞ is the probability that a given node belongs to a supernode with infinite size.

Let us explain the right-hand terms in Eq. 3. The probability that the end node (supernode) of a randomly chosen edge of type i , has degree q_i is $q_i P_m(\mathbf{q}) / \langle q_i \rangle$. There

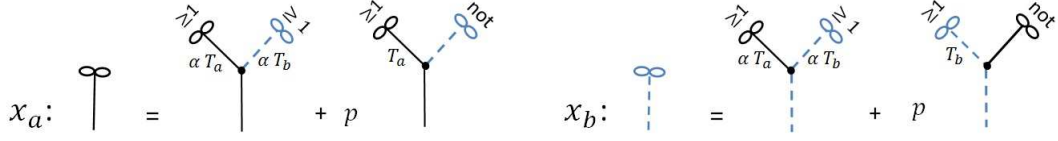


FIG. 1. Schematic representation of the self-consistency equations for the probabilities x_a and x_b . The solid black and dashed blue lines with infinity symbols at one end represent probabilities x_a and x_b , respectively. For the sake of clarity, we do not show the edges leading to finite components, namely probabilities $1 - x_a$ and $1 - x_b$.

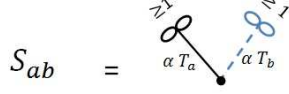


FIG. 2. Schematic representation of the probability that a node belongs to the giant co-infected cluster.

are two possibility: If the end node of the randomly chosen edge of type i , has at least one edge of each type i , which leads to the infected cluster with disease i (probability x_i), the transmissibility of each edge is increased by factor α . The second line of Eq. 3, indicates the contribution of this type of terms. Setting $T_i = 1$ and $\alpha = 1$, these terms are same with those are appeared in deriving of the size of the giant viable clusters [14, 15]. The second possibility is when the end node is only connected to type i of edges, leading to the infinite infected subtree of type i . In this case, there is no cooperation between two diseases. The third line in Eq. 3 is related to this possibility. Notice that these terms do not have any contribution in deriving the giant viable clusters. In order to compare the giant co-infected and the viable clusters, we add the contribution of these terms by factor p , which is equal to one in our co-infection model and is zero for the viable clusters.

Using these probabilities, we can obtain the probability that a randomly chosen node belongs to the giant co-infected cluster, denoted by S_{ab} . This probability, schematically shown in Fig 2, is given by the following expression,

$$S_{ab} = R_\infty + \sum_{m=1}^{\infty} R(m, T_{ab}) \sum_{\mathbf{q}} P_m(\mathbf{q}) \times \left[1 - (1 - \alpha T_a x_a)^{q_a} \right] \left[1 - (1 - \alpha T_b x_b)^{q_b} \right]. \quad (4)$$

We can rewrite Eqs. (3) and (4) in terms of the generating

functions of each network as follows,

$$x_i = R_\infty + \sum_{m=1}^{\infty} R(m, T_{ab}) \times \left(\left[1 - G_1^i(1 - \alpha T_i x_i) \right] \left[1 - G_0^j(1 - \alpha T_j x_j) \right] + p \left[1 - G_1^i(1 - T_i x_i) \right] G_0^j(1 - T_j x_j) \right). \quad (5)$$

and

$$S_{ab} = R_\infty + \sum_{m=1}^{\infty} R(m, T_{ab}) \times \left[1 - G_0^a(1 - \alpha T_a x_a) \right] \left[1 - G_0^b(1 - \alpha T_b x_b) \right]. \quad (6)$$

In which $G_0^i(x)$ and $G_1^i(x)$ are the generating functions for the degree distribution and the excess degree distribution, respectively.

$$G_0^i(x) \equiv \sum_{q_i} P(q_i) x^{q_i}, \quad G_1^i(x) = \sum_{q_i} \frac{q_i P(q_i)}{\langle q_i \rangle} x^{q_i-1}. \quad (7)$$

Index i for the generation functions refers to types of edges $i = a, b$.

B. Erdős–Rényi networks

Let us consider multiplex networks such that each layer is a ER network with $P(k_i) = c_i^{k_i} e^{-c_i k_i} / k_i!$, for $i = a, b$ and $P(k_{ab}) = c_{ab}^{k_{ab}} e^{-c_{ab} k_{ab}} / k_{ab}!$, where $c_i = \langle k_i \rangle$ and $c_{ab} = \langle k_{ab} \rangle$. For ER networks the generating functions are as $G_0(x) = G_1(x) = e^{-c(1-x)}$. Substituting $G_1(x)$ into Eq. (1) we find

$$R(m, T_{ab}) = \frac{(m T_{ab} c_{ab})^{m-1} e^{-m T_{ab} c_{ab}}}{m!}. \quad (8)$$

Also for ER uncorrelated networks, degree distribution of supernodes is given as

$$P_m(\mathbf{q}) = \frac{e^{-m c_a} (m c_a)^{q_a}}{q_a!} \frac{e^{-m c_b} (m c_b)^{q_b}}{q_b!}. \quad (9)$$

For the sake of simplicity, let us consider the symmetric case $T_a = T_b = T$ and $c_a = c_b = c$. Also we assume

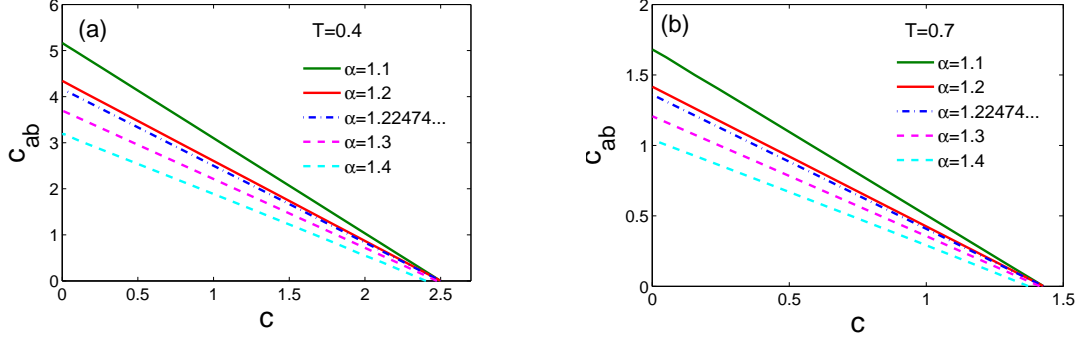


FIG. 3. Lines of transition points for (a) $T = 0.4$ and (b) $T = 0.7$, on the plane (c, c_{ab}) . The solid and dashed lines indicate continuous and discontinuous transition points, respectively. The dotted-dashed line show the line of tricritical points.

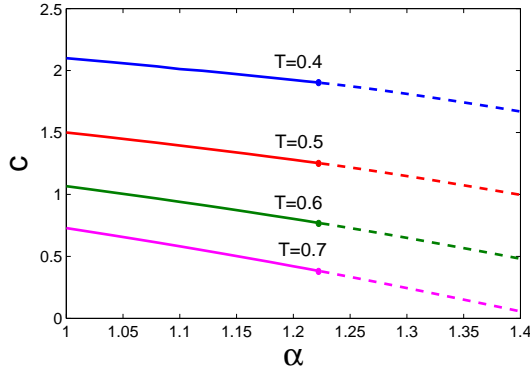


FIG. 4. The phase diagram of the model on ER multiplex network for $c_{ab} = 1$. The dotted lines indicate the position of discontinuous phase transitions while the solid lines show the line of continuous phase transitions. The tricritical point occurs at $\alpha = 1.22474\dots$, for every value of T .

$T_{ab} = \alpha^2 T^2$. In this case, $x_a = x_b \equiv x$, obtained from Eq. (5) for ER networks as,

$$x = R_\infty + \sum_{m=1}^{\infty} R(m, T_{ab}) \times \left[(1 - e^{-m\alpha c T x})^2 + p(1 - e^{-mc T x})e^{-mc T x} \right]. \quad (10)$$

Using Eq. 8, R_∞ is given as

$$\begin{aligned} R_\infty &= 1 - \sum_{m=1}^{\infty} R(m, T_{ab}) \\ &= 1 - \frac{1}{c_{ab} T_{ab}} \sum_{m=1}^{\infty} \frac{(m)^{m-1} (c_{ab} T_{ab} e^{-c_{ab} T_{ab}})^m}{m!} \\ &= 1 + \frac{W(-c_{ab} T_{ab} e^{-c_{ab} T_{ab}})}{T_{ab} c_{ab}}. \end{aligned} \quad (11)$$

In which, $W(x)$ is the Lambert function. Eq. (10) can be simply rewritten in terms of the Lambert function, which enable us to solve the equation analytically,

$$\begin{aligned} x = \Psi(x) &\equiv \\ &1 + \frac{1}{T_{ab} c_{ab}} \left[-W(-c_{ab} T_{ab} e^{-c_{ab} T_{ab} - 2\alpha c T x}) + 2W(-c_{ab} T_{ab} e^{-c_{ab} T_{ab} - \alpha c T x}) \right. \\ &\quad \left. - pW(-c_{ab} T_{ab} e^{-c_{ab} T_{ab} - c T x}) + pW(-c_{ab} T_{ab} e^{-c_{ab} T_{ab} - 2c T x}) \right] \end{aligned} \quad (12)$$

Eq. (12) is a self-consistent equation for x with parameters c, c_{ab}, T and α . To obtain the phase diagram of model, let us define $f(x) \equiv x - \Psi(x)$. Demanding $f(x) = f'(x) = 0$ for $x > 0$, we find the position of dhybrid transitions, while a continuous transition occurs when $f(0) = f'(0) = 0$ and $f''(0) > 0$.

The lines in Fig. (3) show the position of transition points in the plane (c, c_{ab}) , for each values of α . For $\alpha < 1.22474\dots$, we find a line of continuous transition points. As α increases, the type of transition changes and lines indicate the position of hybrid transitions.

Moreover, Fig. (4) shows the phase diagram of the co-

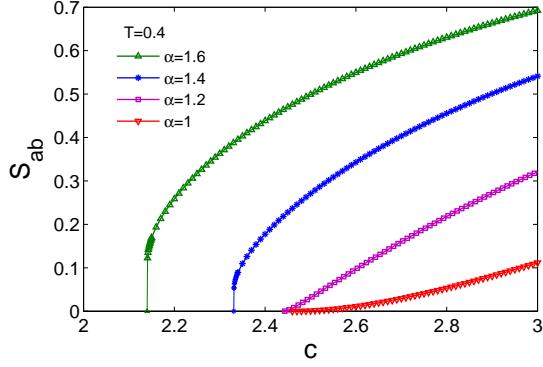


FIG. 5. The relative size of the giant co-infected cluster for $c_{ab} = 0.1$. Each curve corresponds to a different value of cooperativity.

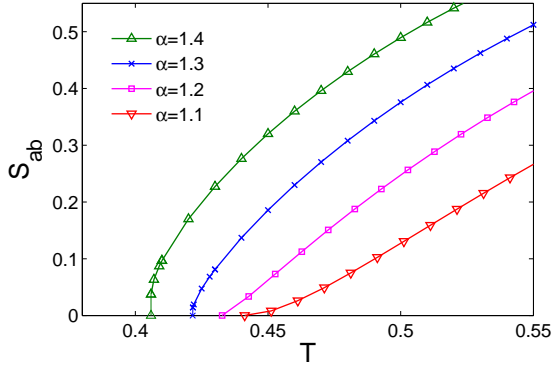


FIG. 6. The relative size of the giant co-infected cluster for $c_{ab} = 0.5$ and $c = 2$ vs transmission probability T . Each curve corresponds to a different value of cooperativity.

infection model, obtained for $c_{ab} = 1$ and for different values of T . For low values of cooperation α , the transition is continuous, while with increasing α , the transition becomes discontinuous. The point $\alpha = 1.22474\dots$ is a tricritical point, determined by solution of $f(0) = f'(0) = f''(0) = 0$.

Following the derivation of Eq. (4), we can obtain the probability that a given node belongs to the giant co-infected cluster:

$$S_{ab} = 1 + \frac{1}{T_{ab}c_{ab}} \left[-W(-c_{ab}T_{ab}e^{-c_{ab}T_{ab}-2\alpha cTx}) + 2W(-c_{ab}T_{ab}e^{-c_{ab}T_{ab}-\alpha cTx}) \right]. \quad (13)$$

We plotted S_{ab} for different values of cooperation α in terms of the mean degree of networks, c and the transmissibility, T in Figs. (5) and (6), respectively. For $\alpha > 1.22474\dots$, the giant co-infected cluster emerges discontinuously at the transition point. As the fraction of

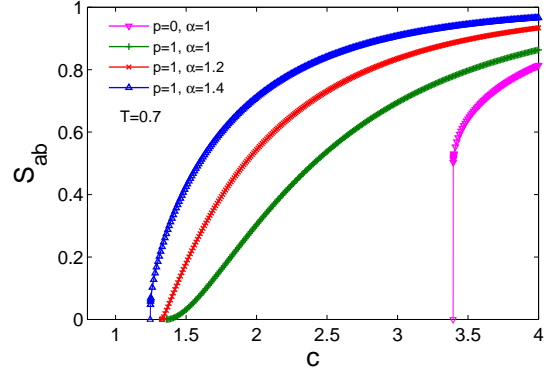


FIG. 7. The relative size of the giant co-infected clusters with ($p = 1, \alpha > 1, T < 1$), compared with the size of the giant viable cluster ($p = 0, \alpha = 1$), in ER multiplex network for $c_{ab} = 0.1$. The curve corresponding with ($p = 1, \alpha = 1$), shows the size of the giant infected cluster without cooperativity.

overlapped edges is decreased, the jump values become smaller. However even for $c_{ab} = 0$, the jump values are not zero and the transitions occur discontinuously. As the cooperativity increases, the epidemic threshold decreases to the smaller values of T or c , which means, cooperation between two diseases decreases the network's robustness against the propagation of both diseases.

At the end, we compare the size of the giant co-infected cluster with the giant viable cluster. In multiplex networks, a viable cluster by definition is a set of nodes in which, for every type of edges, each two nodes are interconnected by at least one path following only (occupied) edges of this type. With this definition, the paths must pass through only the nodes in the cluster. Setting $p = 0, \alpha = 1$ in Eqs. (3) and (4), we can derive the size of the giant viable clusters. It was shown that viable clusters emerge discontinuously for every value of overlapping [33]. Fig. 7 shows the size of the viable cluster, compared with the co-infected clusters. The particular case of ($p = 1, \alpha = 1$), is the overlap area of the giant connected components of two layers with occupied edges of type a and b . The overlapped cluster include the viable cluster, since between each two nodes of the cluster, there is at least one path following each type of occupied edges, but the paths can pass through nodes out of the cluster and then return to the cluster. The overlapped cluster, which corresponds with an infected cluster without cooperativity, emerges continuously. For $\alpha > 1$, cooperation between two diseases occurs and diseases can infect more fraction of the nodes. Increasing the value of α , the size of the co-infected cluster becomes greater. Also, with increasing α , the common terms in deriving of the co-infected and viable clusters, have more contribution. Hence co-infected clusters show hybrid transitions similar with those as seen for the viable clusters.

III. CONCLUSION

In this paper, we have introduced a coinfection model for two diseases spreading on multiplex networks with the edge overlapping. Two diseases can propagate simultaneously on one multiplex network, such that both diseases can infect the same set of nodes. Our model illustrates how the existence of one infectious disease can enhance the propagation of the other disease. Using the generating function technique, we have given an analytic solution for the size of the giant co-infected cluster, i.e. the set of nodes infected with both diseases, for uncorrelated multiplexes with arbitrary degree distribution. We showed that the cooperation of two diseases decreases the network's robustness against propagation of both diseases, such that the epidemic threshold is shifted to the smaller values of edge transmission probability or the mean de-

gree of networks. Our results show that for low cooperativity, the co-infected cluster emerges continuously. However increasing the strength of cooperation, the type of phase transition changes to hybrid. Hence a tricritical point is appeared in our coinfection model. We compared the size of the giant co-infected cluster with the viable cluster for multiplex networks, considering edge overlapping. With increasing cooperativity, the co-infected cluster shows similar behavior like the viable cluster at the emergence point. The viable cluster is a subgraph of the co-infected cluster. However for large infected clusters these two clusters can coincide.

ACKNOWLEDGMENTS

I would like to thank P. Grassberger for useful conversations and his suggestions to improve the manuscript.

-
- [1] C. Kwan, J. Ernst, Clin Microbiol Rev 24(2):351-376 (2011).
 - [2] K. Lacombe et al., Eighth International AIDS Society Conference on HIV Pathogenesis, Treatment, and Prevention (IAS 2015), Vancouver, abstract TUAB0207LB, 2015.
 - [3] J.K. Rockstroh and S. Bhagani, BMC Medicine 11, 234 (2013).
 - [4] J.F. Brundage and G.D. Shanks, Emerg. Infect. Dis. 14, 1193 (2008).
 - [5] D. A. Vascoa, H. J. Wearinga, P. Rohani, Journal of Theoretical Biology 245, 9-25 (2007).
 - [6] M. E. J. Newman, C. R. Ferrario, PLoS ONE, 8 e71321 (2013).
 - [7] L. Chen, F. Ghanbarnejad, W. Cai and P. Grassberger, EPL, 104 50001 (2013).
 - [8] W. Cai, L. Chen, F. Ghanbarnejad and P. Grassberger, NATURE Physics 2015, 3457 (2015).
 - [9] L. Hébert-Dufresne and B.M. Althouse, PNAS 112, 10551 (2015).
 - [10] H. Susi, B. Barre s, P. F. Vale, A.-L. Laine, NATURE Commun. 6 5975 (2015).
 - [11] M. Marv , E. Venturino, R. B. de la Parra, J. of Appl. Math. 2015, 275485, (2015).
 - [12] P. Grassberger, Math. Biosci. 63, 157172 (1982).
 - [13] S. V. Buldyrev, R. Parshani, G. Paul, H. E. Stanley and S. Havlin, Nature 464, 1025 (2010).
 - [14] S.-W. Son, G. Bizhani, C. Christensen, P. Grassberger and M. Paczuski, Europhys. Lett. 97, 16006 (2012).
 - [15] G. J. Baxter, S. N. Dorogovtsev, A. V. Goltsev, and J. F. F. Mendes, Phys. Rev. Lett. 109, 248701 (2012).
 - [16] B. Min and K.-I. Goh, Phys. Rev. E 89, 040802(R) (2014).
 - [17] N. Azimi-Tafreshi, S. N. Dorogovtsev, J. F. F. Mendes, Phys. Rev. E 90, 052809 (2014).
 - [18] P. Grassberger, Phys. Rev. E 91, 062806 (2015).
 - [19] S. Boccaletti, G. Bianconi, R. Criado, C. I. del Genio, J. G mez-Garde es, M. Romance, I. Sendina-Nadal, Z. Wang, and M. Zanin, Phys. Rep. 544, 1 (2014).
 - [20] K.-M. Lee, B. Min, K.-I. Goh, Eur. Phys. J. B, 88 (2015).
 - [21] M. E. J. Newman, Phys. Rev. Lett. 95, 108701 (2005).
 - [22] S. Funk and V. A. A. Jansen, Phys. Rev. E 81, 036118 (2010).
 - [23] S. Funk, E. Gilad, V. A. A. Jansen, J. Theor. Biol. 264, 501509 (2010).
 - [24] B. Karrer and M. E. J. Newman, Phys. Rev. E 84, 036106 (2011).
 - [25] Y. Wang, G. Xiao, J. Liu, New J. Phys. 14 013015 (2012).
 - [26] V. Marceau, P.-A. Noel, L. H bert-Dufresne, A. Allard, L. J. Dub , Phys. Rev. E. 84 026105 (2011).
 - [27] F. Sahneh, C. Scoglio, Phs. Rev. E 89, 062817 (2014).
 - [28] C. Granell, S. G mez, and A. Arenas, Phys. Rev. Lett. 111, 128701 (2013).
 - [29] W. Wang, M. Tang, H. Yang, Y. Do, Y.-Ch. Lai, G. Lee, Nature Scientific Reports, Volume 4, id. 5097 (2014).
 - [30] X. Wei, N. C. Valler, B. A. Prakash, I. Neamtiu, M. Faloutsos, and C. Faloutsos, IEEE J. Sel. Areas Commun. 31, 1049 (2013).
 - [31] Kermack W. O. and McKendrick A. G., Proc. R. Soc. A, 115 700 (1927).
 - [32] M. E. J. Newman, Phys. Rev. E 66, 016128 (2002).
 - [33] Y. Hu, D. Zhou, R. Zhang, Z. Han, Sh. Havlin, Phys. Rev. E 88, 052805 (2013).
 - [34] B. Min, S. Lee, K.-M. Lee, K.-I. Goh, Chaos Solitons Fractals 72, 4958 (2015).
 - [35] M. E. J. Newman, Phys. Rev. E 76, 045101(R) (2007).
 - [36] M. E. J. Newman, S. H. Strogatz, and D. J. Watts, Phys. Rev. E 64, 026118 (2001).
 - [37] M. Z. Bazant, Physica A 316 2955 (2002).